High-Energy Behavior of Quark Non-Local Operator: Implications for Lattice Calculations

Giovanni Antonio Chirilli

University of Salento - Lecce

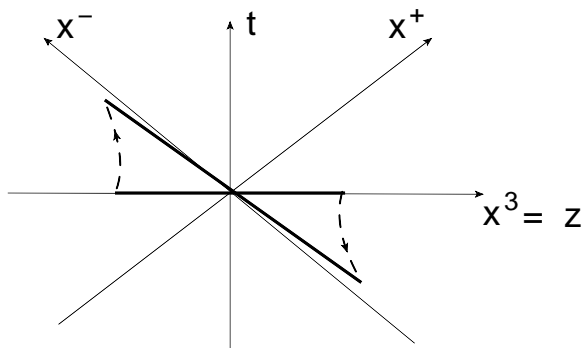Jefferson Lab

Newport News - VA

18 December 2023

- Over the past decade, the investigation of Euclidean-separated, gauge-invariant, bi-local operators via lattice gauge formalism has gained significant interest due to its ability to provide direct access to parton distribution functions (PDFs) from first principles.

- Key observation: space-like separated operators can be examined through lattice QCD formalism. In the infinite momentum frame they reduce to the conventional light-cone operators through which PDFs are defined (X. Ji: 2013).

  ▶ Deviations from the infinite momentum frame emerge as inverse powers of the large parameter of the boost, suggesting that such corrections can be systematically suppressed.

Motivation

- The distributions introduced by Ji, known as quasi-PDFs, were later complemented by alternative PDFs called pseudo-PDFs (Radyushkin: 2017).

- The Bjorken-x (x_B) dependence of these two distributions has been extensively studied in recent years;
  - lattice formalism is unlikely to provide access to their behavior at small x_B values: need to reduce considerably the lattice spacing a in order to access higher energy: $P \sim \frac{1}{a}$

- In view of the future Electron-ion Collider, knowledge of the pseudo- and quasi-PDFs at a wider kinematic regime is desirable.

- We are going to demonstrate that despite being defined through the same space-like separated bi-local operators, quark quasi- and pseudo-PDFs exhibit distinctly different behavior at small x_B values.

Primordial idea

$$\langle P|\bar{\psi}(x^+)\gamma^+[x^+,0]\psi(0)|P\rangle \quad \rightarrow \quad \langle P|\bar{\psi}(z)\gamma^3[z,0]\psi(0)|P\rangle + \mathcal{O}\left(\frac{\Lambda^2}{(P^3)^2}\right)$$

$$x^{\pm} = \frac{x^0 \pm x^3}{\sqrt{2}}$$

JLab/W&M Collaboration
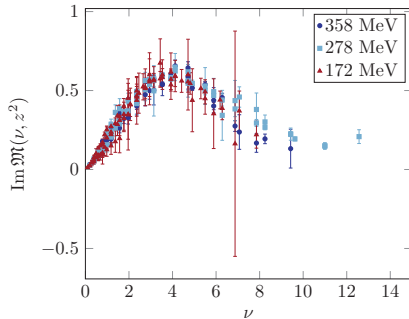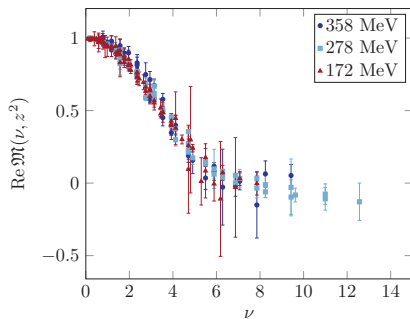
Phys.Rev.Lett. 125 (2020) 23, 232003

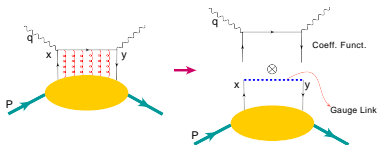Ioffe-time $\nu \equiv z \cdot P$ $\qquad$ z^{μ} space-like vector $\qquad$ $i = 1, 2$

This talk: $\nu \to \varrho$

- Obtain the large behavior of the pseudo Ioffe-time distribution

- Obtain the behavior of the quasi distribution in the same regime

- Compare the Leading and next-to-leading twist contribution with the BFKL resummation result for the pseudo Ioffe-time distribution and also for the quasi distribution

- Compare the small-x_B behavior of the pseudo-PDFs and quasi-PDFs in the Leading and next-to-leading twist approximation and with the BFKL resummation

Number density of quarks

$$x^\mu = n^\mu x^+ + n'^\mu x^- + x_\perp^\mu, \qquad x^\pm = \frac{x^0 + x^3}{\sqrt{2}}, \qquad x_\mu n^\mu = x^- \qquad x_\mu n'^\mu = x^+$$

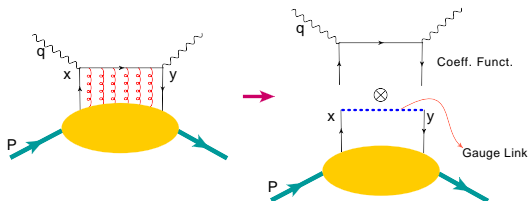$$q(x_B) = \int \frac{d\xi^+}{4\pi} e^{ix_B P^- \xi^-} \langle P | \bar{\psi}(0) \gamma^- \psi(\xi^+ n) | P \rangle$$

- gauge link   restores gauge invariance

$$[0,x] = P \exp\left(-ig \int_0^x ds_\mu A^\mu(s) \right)$$

$$q(x_B) = \int \frac{d\xi^+}{4\pi} e^{ix_B P^- \xi^+} \langle P | \bar{\psi}(0) \gamma^- [0, \xi^+ n] \psi(\xi^+ n) | P \rangle$$
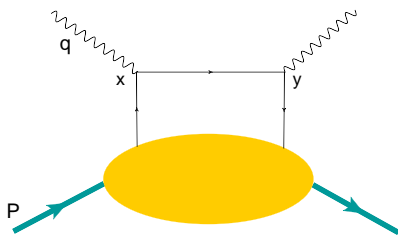
- scale dependence UV divergence
  ⇒ operator have to be renormalized at some scale μ;

$$q(x_B, \mu) = \int \frac{d\xi^+}{4\pi} \, e^{ix_B P^- \xi^+} \langle P | \bar{\psi}(0) \gamma^- [0, \xi^+ n] \psi(\xi^+ n) | P \rangle$$
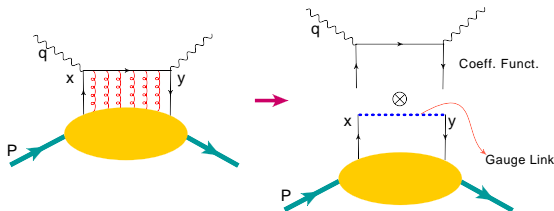
Formal derivation of the quark distribution operator

$$W_{\mu\nu} = \frac{1}{\pi}\text{Im}T_{\mu\nu}$$

$$T_{\mu\nu} = \int d^4x\, e^{iq\cdot x}\langle P|\text{T}\{j_\mu(x)j_\nu(0)\}|P\rangle$$

$$T_{\mu\nu} = \int d^4x\, e^{iq\cdot x} \langle P|\mathrm{T}\{j_\mu(x)j_\nu(0)\}|P\rangle$$

$$T\{j_\mu(x)j_\nu(y)\} = C_\xi^{\mu\nu}(x,y)\, \bar{\psi}(x)\gamma_\mu\gamma^\xi\gamma_\nu[x,y]\psi(y) + O((x-y)^2)$$

- $C_\xi^{\mu\nu}(x,y)$ is the coefficient function calculable in pQCD

- $\bar{\psi}(x)\gamma_\mu\gamma^\xi\gamma_\nu[x,y]\psi(y)$ is the non local operator

$$T_{\mu\nu} = \int d^4x \, e^{iq \cdot x} \langle P|\mathrm{T}\{j_\mu(x)j_\nu(0)\}|P\rangle$$

OPE in light-ray operators $\qquad\qquad\qquad\qquad (x-y)^2 \to 0$
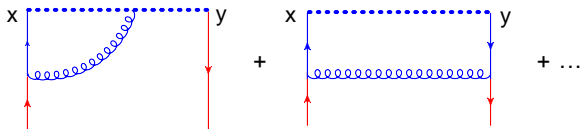
$$T\{j_\mu(x)j_\nu(y)\} = C_\xi^{\mu\nu}(x,y)\,\bar\psi(x)\gamma_\mu\gamma^\xi\gamma_\nu[x,y]\psi(y) + O((x-y)^2)\text{Higher Twist}$$

Higher-Twist $\sim \frac{1}{Q^2}$

Q^2 is the resolution of the probe.

$$[x,y] = \mathrm{P}\exp\left(ig\int_y^x ds_\mu A^\mu(s)\right)$$
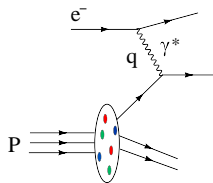
DGLAP evolution equation

Renorm-group equation for light-ray operators

$$\mu^2 \frac{d}{d\mu^2} \bar{\psi}(x)[x,y]\psi(y) \;=\; K_{\mathrm{LO}} \bar{\psi}(x)[x,y]\psi(y) + \ldots$$

DGLAP evolution of parton densities

Incoherent Interactions

Coherent Interactions

VS.

Bjorken Limit

Regge Limit

$$-q^2 = Q^2 \to \infty, \ (P+q)^2 = s \to \infty$$

$$x_{\mathrm{B}} = \frac{Q^2}{s + Q^2} \ \text{fixed}$$

resum $\alpha_s \ln \dfrac{Q^2}{\Lambda_{\mathrm{QCD}}^2}$
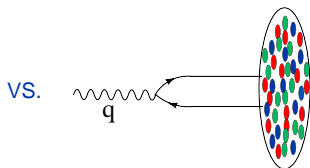
$$Q^2 \ \text{fixed}, \ s \to \infty$$

$$x_{\mathrm{B}} = \frac{Q^2}{s} \to 0$$

resum $\alpha_s \ln \dfrac{1}{x_{\mathrm{B}}}$

At small-x_B, higher twist cannot be neglected.

small-x_B limit of DGLAP equation

The Q^2 behavior of DIS structure function is obtained from the anomalous dimension of twist-two operators

$$\mu \frac{d}{\mu} F^a_{\xi+} \nabla^{n-2}_+ F^{a\ \xi}_+ = K_{gg}(x_B, \alpha_s) \otimes F^a_{\xi+} \nabla^{n-2}_+ F^{a\ \xi}_+$$

$$K^{(0)}_{gg}(x_B, \alpha_s) \underset{x_B \to 0}{\sim} \frac{\bar{\alpha}_s}{x_B} \qquad\qquad \bar{\alpha}_s = \frac{\alpha_s N_c}{\pi}$$

in Mellin space $\quad \int dx_B x_B^{n-1}$

$$\mu \frac{d}{\mu} F^a_{\xi+} \nabla^{n-2}_+ F^{a\ \xi}_+ = \gamma(\alpha_s, n) F^a_{\xi+} \nabla^{n-2}_+ F^{a\ \xi}_+$$

$$\gamma^{(0)}_{gg}(n) \underset{n \to 1}{\sim} \frac{\bar{\alpha}_s}{n-1}$$

$x_B = \frac{Q^2}{s} \to 0$
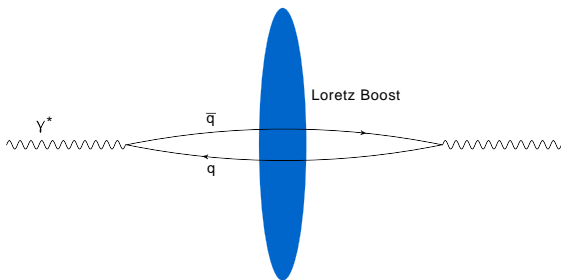
Formation time of the $q\bar{q}$ pair: $t_f \sim \frac{1}{\Delta E} \sim \frac{1}{M x_B}$

Compare with typical partons' interaction time: $t_{int} \sim R_P$
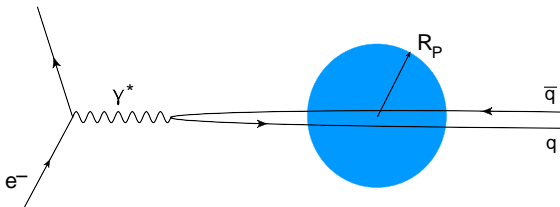
$$\langle P | \mathrm{T}\{J^{\mu}(x) J^{\nu}(y)\} | P \rangle$$
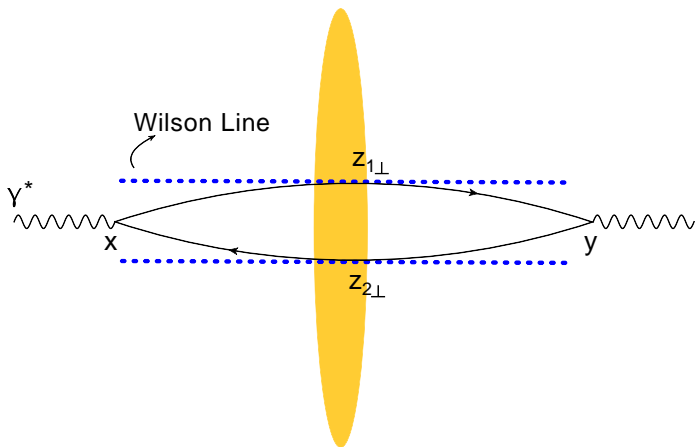
$$\langle P|\mathrm{T}\{J^\mu(x)J^\nu(y)\}|P\rangle = \int d^2z_1 d^2z_2 I^{\mu\nu}(x,y;z_1,z_2)\langle P|\mathrm{Tr}\{U(z_1)U^\dagger(z_2)\}|P\rangle$$

light-cone vectors p_1^μ and p_2^μ

$$U(x_\perp) = \text{Pexp}\left\{ ig \int_{-\infty}^{\infty} du \, p_{1\mu} \, A^\mu(up_1 + x_\perp) \right\}$$

$$n^\mu = p_1^\mu + e^{-2\eta} p_2^\mu$$

$$U^\eta(x_\perp) = \text{Pexp}\left\{ ig \int_{-\infty}^{\infty} du \, n_\mu \, A^\mu(un + x_\perp) \right\}$$

Alternatively use rigid cut-off; useful to preserve conformal invariance in higher order calculations.

$$U^{\eta}(x_{\perp}) = \text{Pexp}\left\{ ig \int_{-\infty}^{\infty} du\, n_{\mu} A^{\mu}(un + x_{\perp}) \right\}$$

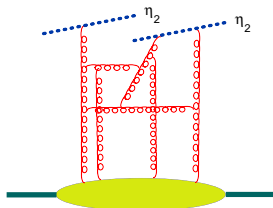$$\langle P|\text{T}\{J^{\mu}(x)J^{\nu}(y)\}|P\rangle = \int d^2z_1 d^2z_2 I^{\mu\nu}(x,y;z_1,z_2)\langle P|\text{Tr}\{U^{\eta}(z_1)U^{\eta\dagger}(z_2)\}|P\rangle$$

$$\frac{d}{d\eta}\mathrm{tr}U^{\eta}(z_1)U^{\eta\dagger}(z_2)\}$$

$$\alpha_s(\eta_1 - \eta_2)K_{\text{evol}} \otimes$$

Non-linear BK evolution equation

$$\hat{\mathcal{U}}(x,y) \equiv 1 - \frac{1}{N_c}\text{tr}\{\hat{U}(x_\perp)\hat{U}^\dagger(y_\perp)\}$$

$$\frac{d}{d\eta}\hat{\mathcal{U}}(x,y) = \frac{\alpha_s N_c}{2\pi^2}\int \frac{d^2z\,(x-y)^2}{(x-z)^2(y-z)^2}\Big\{\hat{\mathcal{U}}(x,z) + \hat{\mathcal{U}}(z,y) - \hat{\mathcal{U}}(x,y) - \hat{\mathcal{U}}(x,z)\hat{\mathcal{U}}(z,y)\Big\}$$

- LLA for DIS in pQCD $\Rightarrow$ BFKL
  - (LLA: $\alpha_s \ll 1, \alpha_s\eta \sim 1$): Ladder type of diagrams: proliferation of gluons.

- LLA for DIS in semi-classical-QCD $\Rightarrow$ BK/JIMWLK eqn
  - background field method: describes recombination process.

electron-proton/nucleus Deep Inelastic Scattering (DIS) $s = (q + P)^2$

$$\langle P | T\, j^\mu(x) j^\nu(y) | P \rangle$$

energy suppressed
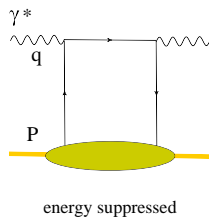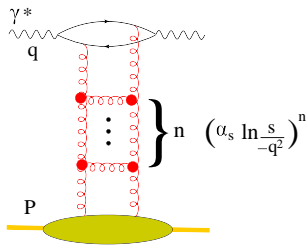
- BFKL resum $\left(\alpha_s \ln \frac{s}{-q^2} \right)^n$

- Dynamics is linear and it describes proliferation of gluons
  $\Rightarrow$ Violation of Unitarity

$$T\{\hat{j}_\mu(x)\hat{j}_\nu(y)\} = \int d^2z_1 d^2z_2 \, I^{\text{LO}}_{\mu\nu}(z_1, z_2, x, y) \text{tr}\{\hat{U}^\eta_{z_1} \hat{U}^{\dagger\eta}_{z_2}\}$$

- Calculate LO Imapct factor: $I^{\text{LO}}_{\mu\nu}(z_1, z_2, x, y)$

- Calculate evolution of matrix element $\text{tr}\{\hat{U}^\eta_{z_1} \hat{U}^{\dagger\eta}_{z_2}\}$
  - we need only linear terms: BFKL;

- Solve the evolution equation with initial condition: GBW/MV model;

- Convolute the solution of the evolution equation with the impact factor.

DIS at high-energy $\quad -q^2 = Q^2 \gg P^2 \qquad s = (P+q)^2 \gg Q^2$

$$\sigma^{\gamma^* p}(x_B, Q^2) = \int d\nu \, F(\nu) \, x_B^{-\aleph(\nu)-1} \left(\frac{Q^2}{P^2}\right)^{\frac{1}{2}+i\nu}$$

$\aleph(\gamma)$ is the BFKL pomeron intercept. $\qquad\qquad \gamma = \frac{1}{2} + i\nu$

Saddle point approximation:

$$\sigma^{\gamma^* p}(x_B, Q^2) \sim \left(\frac{1}{x_B}\right)^{\bar{\alpha}_s 4 \ln 2}$$

n-th moment of the structure function is

$$M_n = \int_0^1 dx_B \, x_B^{n-1} \sigma^{\gamma^* p}(x_B, Q^2) = \int_{\frac{1}{2}-i\infty}^{\frac{1}{2}+i\infty} d\gamma \, \frac{F(\gamma)}{n-1-\aleph(\gamma)} \left(\frac{Q^2}{P^2} \right)^\gamma$$

$$\aleph(\gamma) = \bar\alpha_s \left(2\psi(1) - \psi(\gamma) - \sum_{m=1}^{N} \frac{1}{m-\gamma} - \psi(N+1-\gamma) \right)$$

The BFKL is given as a sum over all the residues

- Leading residue ~ 1: $\quad \aleph(\gamma) \rightarrow \frac{\bar\alpha_s}{\gamma-1}$ $\qquad \bar\alpha_s = \frac{\alpha_s N_c}{\pi}$

- Next-to-Leading residue $\sim \frac{1}{Q^2}$: $\quad \aleph(\gamma) \rightarrow \frac{\bar\alpha_s}{\gamma-2}$

Closing the contour on the poles we get the anomalous dimensions of the leading and higher twist operators at the *unphysical point* $n = 1$.

Analytic continuation in the complex plane

$$\int_0^1 dx_B \, x_B^{n-1} \sigma^{\gamma^* p}(x_B, Q^2) = \int_{\frac{1}{2}-i\infty}^{\frac{1}{2}+i\infty} d\gamma \, \frac{F(\gamma)}{\omega - \aleph(\gamma)} \left(\frac{Q^2}{P^2}\right)^\gamma$$

Analytic continuation: $n - 1 \rightarrow \omega$ complex continuous variable

$\Rightarrow$ Residues $\omega = \aleph(\gamma) \simeq \frac{\bar{\alpha}_s}{\gamma - 1}$;

$\quad$ Leading $-$ Twist $\quad \gamma(\alpha_s, \omega) = \frac{\bar{\alpha}_s}{\omega} + \mathcal{O}(\alpha_s^2), \quad \sigma(\omega, Q^2) \sim \left(\frac{Q^2}{P^2}\right)^{\frac{\bar{\alpha}_s}{\omega}}$

$\alpha_s \ln \frac{1}{x_B} \sim 1 \;\; \rightarrow \frac{\alpha_s}{\omega} \sim 1 \quad x_B \rightarrow 0 \;\Leftrightarrow\; \omega \rightarrow 0 \quad \Rightarrow \quad$ resummation: BFKL eq.

Thus, we get the analytic continuation of anomalous dimension at the *unphysical point* $n \rightarrow 1$ of twist-2 gluon operator $F^a_{\xi+} \nabla^{n-2} F^{\xi a}_{+}$

analytic continuation of local operator to light-ray operators
are singular in the BFKL approximation

$\Rightarrow$ analytic continuation of local operator $F_{\mu_+}^a \nabla_+^{j-2} F_+^{\mu a}$ to
light-ray operators with point-splitting

Wilson frame: gluon operator   Balitsky(2013); Balitsky, Kazakov, Sobko (2013-2015)

quasi-pdf frame: this work (quark and gluon operators)
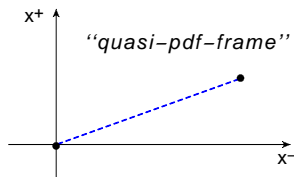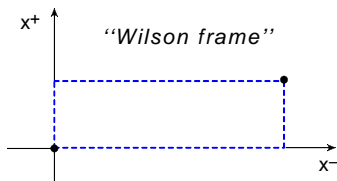
Analytic continuation of light-ray operators at $j = 1$ (or $\omega \to 0$)

$$F_{\xi+}^a(x)\nabla_+^{j-2}F_+^{a\,\xi}(x)\Big|_{x=0} = \frac{\Gamma(2-j)}{2\pi i} \int_0^{+\infty} du\ u^{1-j} F_{\xi+}^a(0)[0,un]^{ab} F_+^{b\,\xi}(un)$$

OPE in light-ray operators in QCD (Balitsky, Braun (1989))

2-point function in BFKL limit (Balitsky; Balitsky, Kazakov, Sobkov (2013-2018))

2-point function in triple Regge limit (Balitsky 2018)

Light-ray operators in CFT (e.g. Kravchuk, Simmons-Duffin (2018))

Lattice calculation of the pseudo-Ioffe-time distribution

Ioffe-time $\varrho \equiv z \cdot P$ $z^2 \neq 0$

$$M^\alpha(z,P) \equiv \langle P|\bar{\psi}(z)\gamma^\alpha[z,0]\psi(0)|P\rangle$$

$$M^\alpha(z,P) = 2P^\alpha \mathcal{M}(\varrho,z^2) + 2z^\alpha \mathcal{N}(\varrho,z^2)$$

- The pseudo-ITD $\mathcal{M}(\varrho,z^2)$ contains (not only) the leading twist term

- $\mathcal{N}(\varrho,z^2)$ contains higher twists terms

- higher twist: $\mathcal{O}(z^2 \Lambda_{QCD})$

- $P = (E,0,0,P^3)$ $z = (0,0,0,z^3)$;
    - for $\alpha = 0$ one isolate $\mathcal{M}(\varrho,z^2)$.

Radyushkin (2017)

Ioffe-time $\varrho \equiv z \cdot P$ $\qquad z^2 \neq 0$

$$M^\alpha(z, P) \equiv \langle P|\bar{\psi}(z)\gamma^\alpha[z, 0]\psi(0)|P\rangle$$

$$M^\alpha(z, P) = 2P^\alpha \mathcal{M}(\varrho, z^2) + 2z^\alpha \mathcal{N}(\varrho, z^2)$$

- Reduced pseudo-ITD removes the UV divergences.

$$\mathfrak{M}(\varrho, z^2) = \frac{\mathcal{M}(\varrho, z^2)}{\mathcal{M}(0, z^2)}$$

- Logarithmic singularity $\ln(-z^2)$ in $\mathfrak{M}(\varrho, z^2)$ (and in $\mathcal{M}(\varrho, z^2)$)
  - $\Rightarrow$ DIS logarithmic scaling violation with respect to the photon virtuality Q^2.

Radyushkin (2017)

Definition of the pseudo and quasi quark PDF

Pseudo Ioffe-time distribution

$$\mathcal{M}(\varrho, z^2) \equiv \frac{z_\mu}{2\varrho} \langle P|\bar{\psi}(z)\gamma^\mu[z,0]\psi(0)|P\rangle$$

Ioffe-time $\varrho \equiv z \cdot P$ z^μ space-like vector $i = 1, 2$

- Large Longitudinal boost

$x^+ \to \lambda x^+, \quad x^- \to \frac{1}{\lambda}x^- \quad x_\perp \to x_\perp$

Ioffe-time distribution at high energy

$$\langle P|\bar{\psi}(L, x_\perp)\gamma^-[Ln^\mu + x_\perp, 0]\psi(0)|P\rangle$$

$\Rightarrow$ At high-energy the Ioffe-time distribution becomes a light-ray operator

$\Rightarrow$ Study the high-energy behavior of the Ioffe-time distribution through the high-energy OPE

Definition of the pseudo and quasi quark PDF

Ioffe-time $\varrho \equiv z \cdot P$ z^μ space-like vector $i = 1, 2$

Pseudo-PDF: Fourier transform with respect to P keeping its orientation fixed
A. Radyushkin (2017)

$$Q_p(x_B, z^2) = \int \frac{d\varrho}{2\pi} \, e^{-i\varrho x_B} \mathcal{M}(\varrho, z^2)$$

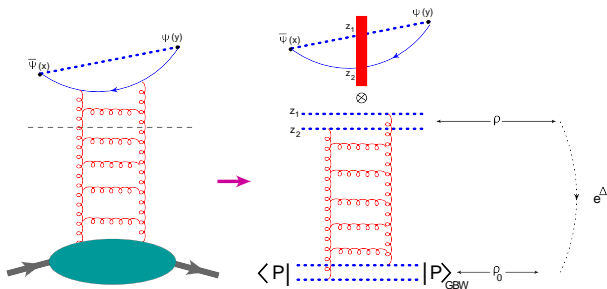Quasi-PDF: Fourier transform with respect to z keeping its orientation fixed
X. Ji (2013)

$$Q_q(x_B, P_\xi) = P_\xi \int \frac{d\varsigma}{2\pi} \, e^{-i\varsigma \, P_\xi x_B} \mathcal{M}(\varsigma P_\xi, \varsigma^2)$$
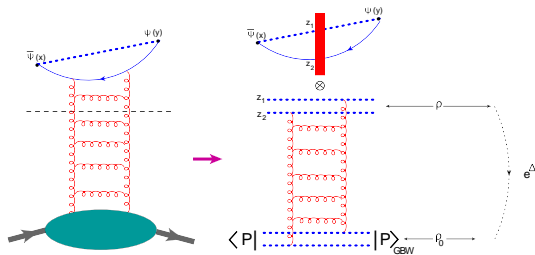
$\xi^\mu = \frac{z^\mu}{|z|}$ $P_\xi = P \cdot \xi$

$$\langle P|\bar{\psi}(x)\gamma^-[x,0]\psi(0)|P\rangle = \int d^2z_2 d^2z_z\, I_q(z_1,z_2;x)\langle P|\mathrm{tr}\{U(z_1)U^\dagger(z_2)\}|P\rangle$$

- Calculate coefficient functions (impact factors) I_q

- Convolute them with the solution of the evolution equation of relative matrix elements

High-energy operator product expansion

$$\mathcal{V}(z_1, z_2) = \frac{1}{z_{12}^2}\left(1 - \frac{1}{N_c}\text{tr}\{U_{z_1}U_{z_2}^\dagger\}\right)$$

Resum $\alpha_s \ln \varrho$ with BFKL eq.

$$a = -\frac{2x^+y^+}{(x-y)^2 a_0}$$

$$2a\frac{d}{da}\mathcal{V}_a(z_\perp) = \frac{\alpha_s N_c}{\pi^2}\int d^2z'\left[\frac{\mathcal{V}_a(z'_\perp)}{(z-z')_\perp^2} - \frac{(z,z')_\perp \mathcal{V}_a(z_\perp)}{z'^2_\perp(z-z')_\perp^2}\right]$$

solution

$$\mathcal{V}^a(z_{12}) = \int \frac{d\nu}{2\pi^2}(z_{12}^2)^{-\frac{1}{2}+i\nu}\left(\frac{a}{a_0}\right)^{\frac{\aleph(\gamma)}{2}}\int d^2\omega(\omega_\perp^2)^{-\frac{1}{2}-i\nu}\mathcal{V}^{a_0}(\omega_\perp)$$
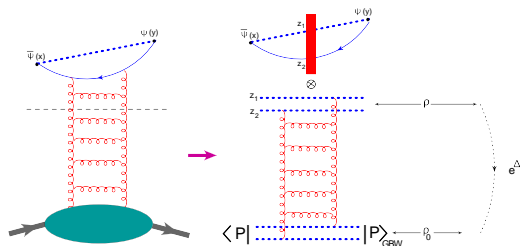
Saddle point approximation

$$\mathcal{M}(\varrho, z^2) \simeq \frac{i N_c}{64} \frac{Q_s \sigma_0}{|z|} \frac{e^{-\frac{\ln^2 \frac{Q_s|z|}{2}}{7\zeta(3)\bar{\alpha}_s \ln\left(\frac{2\varrho^2}{z^2 M_N^2} + i\epsilon\right)}}}{\sqrt{7\zeta(3)\bar{\alpha}_s \ln\left(\frac{2\varrho^2}{z^2 M_N^2} + i\epsilon\right)}} \left(\frac{2\varrho^2}{z^2 M_N^2} + i\epsilon\right)^{\bar{\alpha}_s 2 \ln 2}$$

saturation scale Q_s, $\quad \sigma_0 = 29.1\,\mathrm{mb}$, $\quad M_N$ mass of the nucleon

Pseudo Ioffe-time distribution at LT and NLT approximation

$$\frac{1}{2\pi i} \int_{1-i\infty}^{1+i\infty} d\omega \, L^{\omega} \int_{x_{\perp}^2 M_N}^{+\infty} dL \, L^{-j} \frac{1}{2P^{-}} \langle P | \bar{\psi}(L, x_{\perp}) \gamma^{-} [nL + x_{\perp}, 0] \psi(0) | P \rangle$$

$$= \frac{i N_c Q_s^2 \sigma_0}{24\pi^2 \bar{\alpha}_s} \left(\frac{4\bar{\alpha}_s \left| \ln \frac{Q_s |z|}{2} \right|}{\ln \left(\frac{2\varrho^2}{z^2 M_N^2} + i\epsilon \right)} \right)^{\frac{1}{2}} I_1(u) \left(1 + \frac{Q_s^2 |z|^2}{5} \right) + \mathcal{O} \left(\frac{Q_s^4 |z|^4}{16} \right)$$

$$u = \left[4\bar{\alpha}_s \left| \ln \frac{Q_s |z|}{2} \right| \ln \left(\frac{2\varrho^2}{z^2 M_N^2} + i\epsilon \right) \right]^{\frac{1}{2}}$$

$I_1(u)$ is the modified Bessel function of 1st kind.

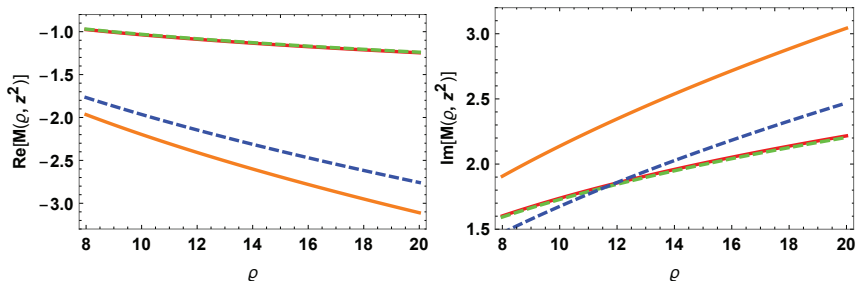# Pseudo Ioffe-time distribution: leading twist vs BFKL resummation

Figure : In the left and right panel we plot the real and imaginary part, respectively of the Ioffe-time amplitude; we compare the numerical evaluation (orange curve) with its saddle point approximation (blue dashed curve), with the LT, (green dashed curve), and the NLT (red solid curve). To obtain the plots we used $|z| = 0.5$, and $M_N = 1$ GeV.

JLab/W&M Collaboration
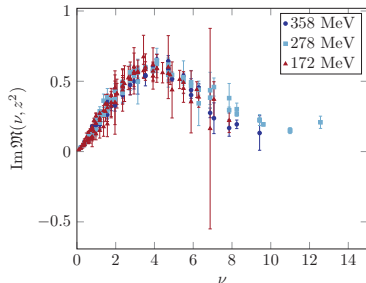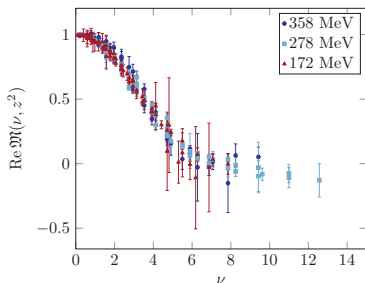
Phys.Rev.Lett. 125 (2020) 23, 232003

Ioffe-time $\nu \equiv z \cdot P$ z^μ space-like vector $i = 1, 2$

This talk: $\nu \to \varrho$

Large Ioffe-time behavior is governed by higher-twists contributions which are not capture by Lattice calculation

Quasi-distribution in the BFKL approximation

$$Q_q(x_B, P_\xi) = P_\xi \int \frac{d\varsigma}{2\pi} \, e^{-i\varsigma \, P_\xi x_B} \mathcal{M}(\varsigma P_\xi, \varsigma^2)$$

$$\xi^\mu = \frac{z^\mu}{|z|} \qquad P_\xi = P \cdot \xi$$

$$\mathcal{M}(\varsigma P_\xi, \varsigma^2) = \frac{1}{2P_\xi} \langle P | \bar{\psi}(\varsigma) \slashed{g}[\varsigma, 0] \psi | P \rangle$$

Saddle point approximation for the quasi-distribution

$$\mathcal{M}(\varsigma P_\xi, \varsigma^2) \simeq \frac{i N_c Q_s \sigma_0}{64|\varsigma|} \frac{e^{-\frac{\ln^2 \frac{Q_s|\varsigma|}{2}}{7\zeta(3)\bar{\alpha}_s \ln\left(-\frac{2P_\xi^2}{M_N^2} + i\epsilon\right)}}}{\sqrt{7\zeta(3)\bar{\alpha}_s \ln\left(-\frac{2P_\xi^2}{M_N^2} + i\epsilon\right)}} \left(-\frac{2P_\xi^2}{M_N^2} + i\epsilon\right)^{\bar{\alpha}_s 2 \ln 2}$$

Quasi-distribution at LT and NLT approximation

$$\frac{1}{2\pi i} \int_{1-i\infty}^{1+i\infty} d\omega \, \varsigma^{\omega} \int_{x_\perp^2 M_N}^{+\infty} d\varsigma \, \varsigma'^{-j} \mathcal{M}(\varsigma P_\xi, \varsigma^2)$$

$$= \frac{iN_c Q_s^2 \sigma_0}{24\pi^2 \bar{\alpha}_s} \left(\frac{4\bar{\alpha}_s \ln \frac{2}{Q_s|\varsigma|}}{\ln \left(-\frac{2P_\xi^2}{M_N^2} + i\epsilon \right)} \right)^{\frac{1}{2}} I_1(\tilde{u}) \left(1 + \frac{Q_s^2 \varsigma^2}{5} \right)$$

with

$$\tilde{u} = \left[4\bar{\alpha}_s \ln \frac{2}{Q_s|\varsigma|} \ln \left(-\frac{2P_\xi^2}{M_N^2} + i\epsilon \right) \right]^{\frac{1}{2}}$$
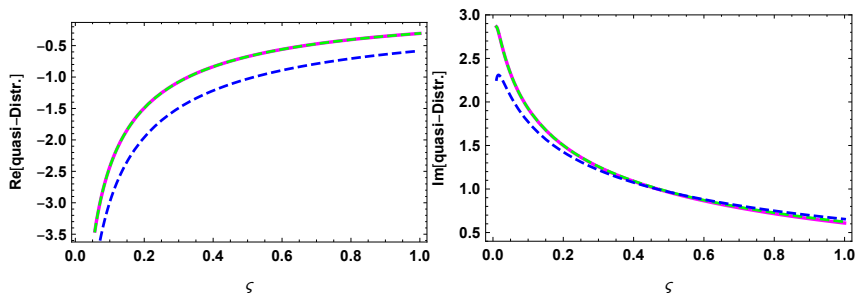
Figure : In the left and right panel we plot the real and imaginary part, respectively, of the quasi-distribution; we compare the numerical evaluation with its saddle point approximation (blue dashed curve).

Pseudo-PDF: Fourier transform with respect to $z \cdot P$

$$Q_{\mathrm{p}}(x_B, z^2) = \int \frac{d\varrho}{2\pi} \, e^{-i\varrho \, x_B} \mathcal{M}(\varrho, z^2)$$

Saddle point approximation

$$Q_{\mathrm{p}}(x_B, z^2) \simeq -\frac{i \, N_c Q_s \sigma_0 \bar{\alpha}_s \ln 2}{32 |z| |x_B|} \frac{e^{\frac{-\ln^2 \frac{Q_s |z|}{2}}{7\zeta(3)\bar{\alpha}_s \ln\left(\frac{2}{x_B^2 z^2 M_N^2} + i\epsilon\right)}}}{\sqrt{7\zeta(3)\bar{\alpha}_s \ln\left(\frac{2}{x_B^2 z^2 M_N^2} + i\epsilon\right)}} \left(\frac{2}{x_B^2 z^2 M_N^2} + i\epsilon\right)^{\bar{\alpha}_s 2 \ln 2}$$

Leading and next-to-leading twist

$$Q_{\mathrm{p}}(x_B, z^2) \simeq \frac{Q_s^2 \sigma_0}{24\pi^2 \alpha_s x_B} \left(\frac{\bar{\alpha}_s \left| \ln \frac{Q_s |z|}{2} \right|}{\ln \left(\frac{2}{x_\perp^2 x_B^2 M_N^2} \right)} \right)^{\frac{1}{2}} \left(1 + \frac{Q_s^2 z^2}{5} \right) I_1(v)$$

$$v \equiv \left[4\bar{\alpha}_s \left| \ln \frac{Q_s |z|}{2} \right| \ln \left(\frac{2}{z^2 x_B^2 M_N^2} \right) \right]^{\frac{1}{2}}$$

Higher twist are suppressed as $z \to 0$

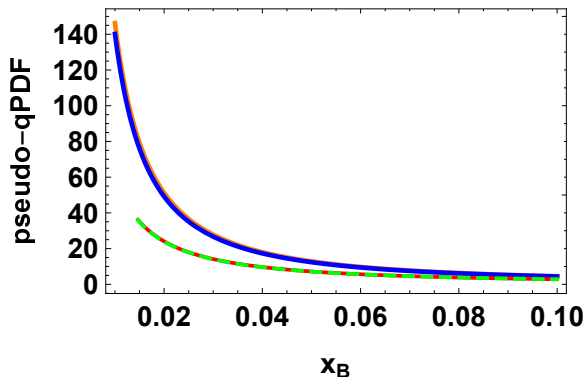# Pseudo quark PDF: leading twists vs BFKL resummation

Figure : The plot presents the quark pseudo PDF by comparing the numerical evaluation (illustrated by the orange curve) with its saddle point approximation (portrayed by the blue curve). Furthermore, we display the leading twist (LT) (marked by the green dashed curve) and the next-to-leading twist (NLT) (signified by the solid red curve).

Quasi-PDF: Fourier transform with respect to z^μ keeping its orientation fixed

$$Q_q(x_B, P_\xi) = P_\xi \int \frac{d\varsigma}{2\pi} e^{-i\varsigma P_\xi x_B} \mathcal{M}(\varsigma P_\xi, \varsigma^2)$$

$\xi^\mu = \frac{z^\mu}{|z|}$ $\qquad P_\xi = P \cdot \xi$

$$Q_q(x_B, P_\xi) \simeq \frac{i N_c P_\xi Q_s \sigma_0}{64\pi} \left(-\frac{2P_\xi^2}{M_N^2} + i\epsilon \right)^{\bar{\alpha}_s 2 \ln 2}$$

$$\times \int_{-\infty}^{+\infty} \frac{d\varsigma}{|\varsigma|} e^{-i\varsigma P_\xi x_B} \frac{e^{-\frac{\ln^2 \frac{Q_s|\varsigma|}{2}}{7\zeta(3)\bar{\alpha}_s \ln\left(-\frac{2P_\xi^2}{M_N^2}+i\epsilon\right)}}}{\sqrt{7\zeta(3)\bar{\alpha}_s \ln\left(-\frac{2P_\xi^2}{M_N^2} + i\epsilon\right)}}$$
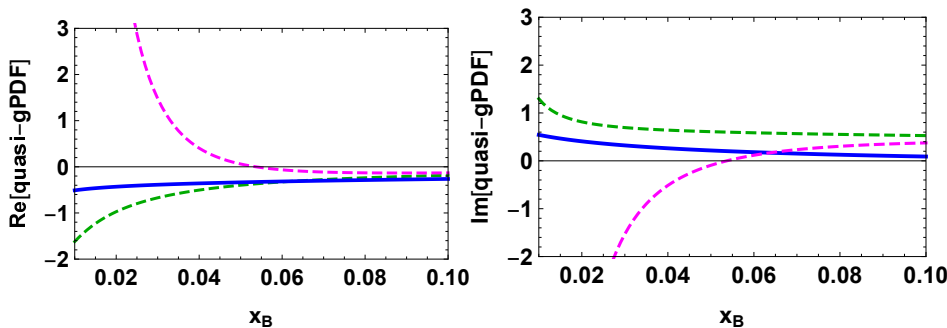
Leading + next-to-leading twist

$$Q_{\mathsf{q}}(x_B, P_\xi) \simeq -\frac{N_c Q_s^2 \sigma_0}{48\pi^3 \bar{\alpha}_s} \frac{1}{x_B} \left(\frac{2\bar{\alpha}_s \ln\left(-\frac{Q_s^2}{4P_\xi^2 x_B^2} - i\epsilon\right)}{\ln\left(-\frac{2P_\xi^2}{M_N^2} + i\epsilon\right)} \right)^{\frac{1}{2}} J_1(t) \left(1 - \frac{2Q_s^2}{5P_\xi^2 x_B^2}\right)$$

Usual exponentiation of the BFKL pomeron intercept, which resums logarithms of x_B, is missing.

For low values of x_B and fixed values of P these corrections are enhanced rather than suppressed at this regime.

quasi quark PDF

Here $P_\xi = 4$ GeV.

The left and right plots show the real and imaginary parts respectively. The Blue curves are the BFKL resummed results, the Green and magenta are the LT and NLT results respectively.

Quasi-PDF have rather unusual behavior at low-x_B.

Conclusions

- Large-distance behavior of the gluon and quark Ioffe-time distribution is computed
  - Ioffe-time ϱ acts as rapidity parameter.
    - $\alpha_s \ln \varrho$ resumed by BFKL eq.

- Pseudo-PDF and quasi-PDF have a very different behavior at low-x_B.
  - pseudo-PDF have typical rising behavior at low-x_B.
  - quasi-PDF have rather unusual behavior at low-x_B.
    - usual exponentiation of the BFKL pomeron intercept, which resums logarithms of x_B, is missing.

- The power corrections in the quasi-PDF do not come in as inverse powers of P but as inverse powers of $x_B P$
  - for low values of x_B and fixed values of P these corrections are enhanced rather than suppressed at this regime.